Dynamic state of DNA topology is essential for genome condensation in bacteria

Ryosuke L Ohniwa[1,*], **Kazuya Morikawa**[2], **Joongbaek Kim**[1], **Toshiko Ohta**[2], **Akira Ishihama**[3], **Chieko Wada**[1] **and Kunio Takeyasu**[1]

[1]Laboratory of Plasma Membrane and Nuclear Signaling, Kyoto University Graduate School of Biostudies, Kitashirakawa Oiwake-cho, Sakyo-ku, Kyoto, Japan; [2]Institute of Basic Medical Sciences, Graduate School of Comprehensive Human Sciences, University of Tsukuba, Tennoh-dai, Tsukuba, Japan and [3]Department of Frontier Bioscience, Hosei University, Koganei, Tokyo, Japan

In bacteria, Dps is one of the critical proteins to build up a condensed nucleoid in response to the environmental stresses. In this study, we found that the expression of Dps and the nucleoid condensation was not simply correlated in *Escherichia coli*, and that Fis, which is an *E. coli* (gamma-Proteobacteria)-specific nucleoid protein, interfered with the Dps-dependent nucleoid condensation. Atomic force microscopy and Northern blot analyses indicated that the inhibitory effect of Fis was due to the repression of the expression of Topoismerase I (Topo I) and DNA gyrase. In the Δ*fis* strain, both *topA* and *gyrA/B* genes were found to be upregulated. Overexpression of Topo I and DNA gyrase enhanced the nulceoid condensation in the presence of Dps. DNA-topology assays using the cell extract showed that the extracts from the Δ*fis* and Topo I-/DNA gyrase-overexpressing strains, but not the wild-type extract, shifted the population toward relaxed forms. These results indicate that the topology of DNA is dynamically transmutable and that the topology control is important for Dps-induced nucleoid condensation.

*Corresponding author. Laboratory of Plasma Membrane and Nuclear Signaling, Kyoto University Graduate School of Biostudies, Kyoto University, Kitashirakawa Oiwake-cho, Sakyo-ku, Kyoto 606-8502, Japan. Tel./Fax: +81 75 753 7905; E-mail: ohniwa@lif.kyoto-u.ac.jp

Introduction

It is intriguing that very long genomic DNA molecules ranging from ∼cm to ∼m (corresponding to ∼10^6 to ∼10^9 base pairs) are stored in small containers with ∼µm in diameter. Two strategies have been taken in the evolution of life to accommodate the genomes in cells: in bacteria, the genomic DNA is packed in a cell as a form of 'nucleoid' (Robinow and Kellenberger, 1994; Poplawski and Bernander, 1997; Azam et al, 2000), whereas, in eukaryotic cells, the genomic DNA exists in a form of chromatin and is packed in a nucleus (Kornberg, 1974; Thoma et al, 1979; Widom and Klug, 1985). In either case, to organize the DNA into higher-order structures, a set of distinct structural DNA-binding proteins, such as histones in eukaryotic cells and Hu in bacteria, constitutively play major roles by utilizing the physical/chemical properties of DNA–protein interactions. A number of additional proteins, such as SMC (structural maintenance of chromosome) proteins and topoisomerases, also play crucial roles in the construction, maintenance and re-construction of well-organized higher-order structures of genomes (Hayat and Mancarella, 1995; Swedlow and Hirano, 2003).

The formation of the higher order structures itself has a biological significance in the protection of the genomic DNA against the environmental stresses. In eukaryotes, DNA damage caused by UV light or oxidative stress accumulate less in nucleosomes than in naked DNA (Ljungman, 1991; Ljungman and Hanawalt, 1992; Yoshikawa et al, 2006). Furthermore, the formation of higher order chromatin dramatically decreases the DNA damage (Ljungman, 1991; Ljungman and Hanawalt, 1992).

In bacteria, one of the proteins to transform the nucleoid into condensed state is Dps (DNA-binding protein from starved cells) (Almiron et al, 1992). Dps is a stress-induced protein with a molecular weight of 19 kDa and is known to be a member of the Fe-binding protein family that forms dodecameric complex in cells (Grant et al, 1998). Dps protects genomic DNA against oxidative stress (Martinez and Kolter, 1997), nuclease cleavage, UV light, thermal shock (Nair and Finkel, 2004) and acid (Choi et al, 2000), possibly by its DNA-binding ability to block the stress elements that attack DNA. Its Fe-chelating activity is also the important feature in the oxidative stress resistance, because iron (Fe^{2+}) supplies an electron to produce the hydroxyl radicals via Fenton reaction (Zhao et al, 2002) and these radicals damage various critical macromolecules including the genomic DNA (Nunoshiba et al, 1999). Dps can reduce the intracellular level of Fe^{2+} and thus restricts the production of hydroxyl radicals (Zhao et al, 2002).

Interaction between DNA and Dps results in a DNA–Dps co-crystal both *in vitro* and *in vivo*. *In vitro*, the mixture of naked DNA and Dps rapidly induces the crystalline state (Wolf et al, 1999; Frenkiel-Krispin et al, 2001). In *Escherichia coli*, Dps becomes the most abundant nucleoid component in the stationary phase (Azam and Ishihama, 1999) and causes a condensation of nucleoid (Wolf et al, 1999; Frenkiel-Krispin et al, 2001; Kim et al, 2004). Electron microscopy observations have revealed that the nucleoid in the stationary phase forms the biocrystal that is composed of the toroidally assembled Dps and DNA (Wolf et al, 1999; Frenkiel-Krispin et al, 2001, 2004). Even after the lysis of the cell, the nucleoid in the stationary phase is in a tightly condensed state (Kim et al, 2004).

The effect of Dps on the nucleoid state can vary depending on the growth conditions or on the bacterial species. The overexpression of Dps in the log phase *E. coli* induces neither nucleoid condensation nor DNA–Dps co-crystallization (Frenkiel-Krispin *et al*, 2001), whereas Dps overexpression in the stationary phase caused nucleoid condensation (Kim *et al*, 2004). In contrast, the nucleoid in *Staphylococcus aureus* transforms its structure into a condensed state in both log and stationary phases by the induction of *mrgA*, a staphylococcal ortholog of *dps* (Morikawa *et al*, 2006). In addition, in *S. aureus*, the oxidative stress promotes the expression of MrgA and nucleoid condensation (Morikawa *et al*, 2006), whereas, in *E. coli*, as shown in this article, an induction of Dps by oxidative stress in the log phase did not result in the condensation of the nucleoid. Based on these differences between *E. coli* and *S. aureus*, we can postulate the presence of additional factors regulating the nucleoid condensation in *E. coli*.

In this study, we show that Fis is the factor inhibiting the nucleoid condensation in the log phase. Fis is abundant in the log phase and is one of the major DNA-binding nucleoid proteins (Azam and Ishihama, 1999). It also acts as a transcription factor (Nilsson *et al*, 1990; Ross *et al*, 1990; Xu and Johnson, 1995; Hengen *et al*, 1997) to regulate a variety of genes. Our analyses show that Fis is one of the specific protein in gamma-Proteobacteria including *E. coli* and is not present in *S. aureus*, and that topoisomerase I (TopoI) and DNA gyrase, which are under the control of Fis in *E. coli*, facilitate the nucleoid condensation. Since Fis, Topo I and DNA gyrase can change the DNA superhelicity (Schneider *et al*, 1997; Schneider *et al*, 1999; Weinstein-Fischer *et al*, 2000), we propose that the control of DNA topology by these proteins is critical for the Dps-induced nucleoid condensation.

Results

Dps expression in E. coli

Two different transcription factors are involved in the *dps*-gene regulation in *E. coli* (Figure 1A). First, IHF controls the accumulation of Dps in the stationary phase (Altuvia *et al*,
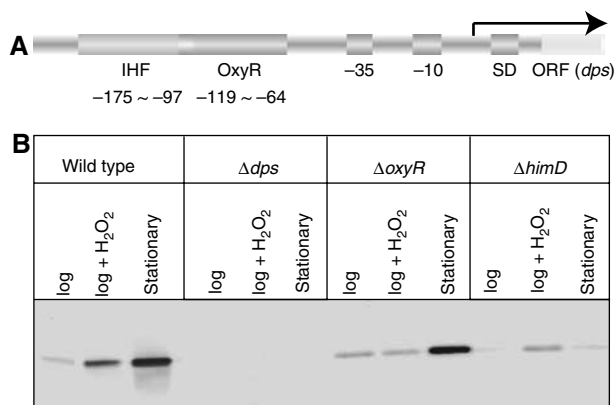
1994; Lomovskaya *et al*, 1994). Second, OxyR, an LysR-family transcription regulator, upregulates the *dps* gene under oxidative stress (such as in the presence of hydrogen peroxide (H_2O_2)) (Altuvia *et al*, 1994; Lomovskaya *et al*, 1994). Our Western blot analysis of wild-type (wt) *E. coli* showed that the levels of Dps expression in the stationary phase and under the oxidative stress were about 10 times and three times higher than that in the log phase, respectively (Figure 1B). On the other hand, in the Δ*dps* strain lacking the *dps* gene, Dps was never detected under all the conditions examined (Figure 1B). In the Δ*oxyR* strain that lacks the *oxyR* gene, the expression of Dps stayed unchanged even after exposure to the oxidative stress, but was highly induced in the stationary phase (Figure 1B). A deletion of *ihf* (Δ*himD*) diminished the induction of Dps during the transition into the stationary phase, but it still allowed the Dps induction under oxidative stress (Figure 1B). Thus, we conclude that the mechanisms of transcriptional regulation of *dps* gene are intact and physiologically functional in our experimental system.

Correlation between the Dps expression and the nucleoid condensation

We have developed 'on-substrate lysis' procedure (see Materials and methods) for removing the cellular membrane and subsequent direct observation of the bacterial nucleoid and eukaryotic chromatin in cells by atomic force microscopy (AFM) (Yoshimura *et al*, 2003; Kim *et al*, 2004). This procedure can be applicable to evaluate the efficiency of nucleoid condensation in *E. coli*, because not-condensed nucleoid extends fibrous structures around the lysed cell, whereas the condensed nucleoid cannot release fibers upon lysis (Kim *et al*, 2004; Morikawa *et al*, 2006). In this study, to elucidate the regulatory factors involved in the Dps-induced nucleoid condensation in *E. coli*, we first assessed the degree of nucleoid condensation under various conditions that induced the Dps expression.

After 'on-substrate lysis', the state of the nucleoid was observed by 4′,6-diamino-2-phenylindole (DAPI) staining. The number of DAPI-stained cells whose nucleoids remained compacted or spread out of the cell (termed 'lysed') was counted, and used as an indication of the degree of the nucleoid condensation. In the log phase, 95 and 93% of the wt and Δ*dps* cells, respectively, were lysed and appeared to have a non-condensed nucleoid (Figure 2A, B and H). Close observations by AFM demonstrated the existence of nucleoid fibers around the lysed cells (Figure 2C and I). In the stationary phase, only 12% of the wt cells were lysed (i.e. condensed) (Figure 2 A, F and G). Although 44% of the Δ*dps* cells were not apparently lysed (Figure 2A), dispersed nucleoid fibers were still observed in the Δ*dps* strain (Figure 2L and M). Namely, the nucleoid becomes condensed during the transition into the stationary phase in a Dps-dependent manner.

In contrast, the oxidative stress given in the log phase induced the expression of Dps but did not condense the nucleoid. Eighty-five percent of the wt cells were efficiently lysed even after the induction of Dps by 2 mM H_2O_2, and the nucleoid fibers were observed around the lysed cells (Figure 2A, D and E). Negative control strains, Δ*dps* and Δ*oxyR* strains, exhibited 81 and 72% efficiency of lysis after the treatment with H_2O_2, respectively (Figure 2A, J, K, P and Q). Therefore, we concluded that the induction of Dps by

Figure 1 Dps expression under different growth conditions. (**A**) Schematic representation of the promoter region of the *dps* gene in *E. coli*. The IHF and OxyR binding sites exist upstream of the −35/−10 sequences (promoter of *dps* gene). (**B**) Western blot analyses against Dps in the wt (W3110) and the W3110 derived Δ*dps*, Δ*oxyR* and Δ*himD* strains, under oxidative stress (2 mM H_2O_2 treatment) in the log phase and in the stationary phase.
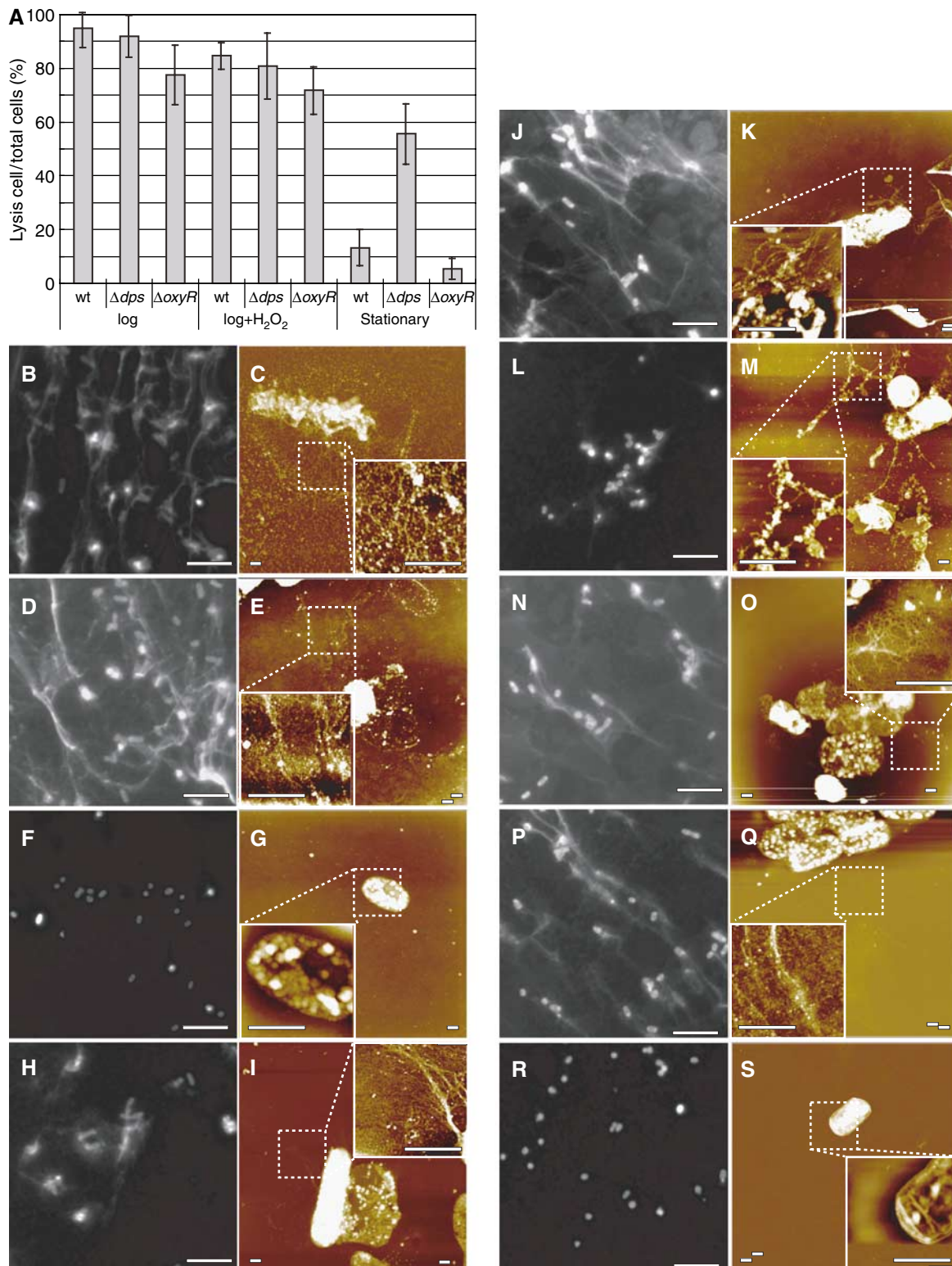
Figure 2 The lysis efficiencies and the nucleoid architectures of the wt, Δ*dps* and Δ*oxyR* strains under three different conditions. (**A**) The efficiency of lysis. The number of lysed cells that dispersed fibers was divided by the total cell number and indicated as percent. The cells were observed by DAPI staining (B, D, F, H, J, L, N, P, R) or by AFM (C, E, G, I, K, M, O, Q, S). The numbers of the cells examined are following (each value separated by slash in parentheses represents the number of cells counted at each independent experiment); wt in log phase (218/154/64/34/54), wt under 2 mM H_2O_2 (235/77/51/135), wt in stationary phase (72/43/109), Δ*dps* strain in the log phase (73/88/17/26), Δ*dps* strain under 2 mM H_2O_2 (102/91/52), Δ*dps* strain in the stationary phase (37/62/75), Δ*oxyRs* strain in the log phase (77/47/51/50), Δ*dps* strain under 2 mM H_2O_2 (74/49/30/53/39), Δ*dps* strain in the stationary phase (74/138/98/165/106). (**B, C**) wt in the log phase, (**D, E**) wt in the log phase treated with 2 mM H_2O_2, (**F, G**) wt in the stationary phase, (**H, I**) Δ*dps* strain in the log phase, (**J, K**) Δ*dps* strain in the log phase treated with 2 mM H_2O_2, (**L, M**) Δ*dps* strain in the stationary phase, (**N, O**) Δ*oxyR* strain in the log phase, (**P, Q**) Δ*oxyR* strain in the log phase treated with 2 mM H_2O_2, (**R, S**) Δ*oxyR* strain in the stationary phase. Scale bars: 10 μm (B, D, F, H, J, L, N, P, R) and 500 nm (C, E, G, I, K, M, O, Q, S).

oxidative stress does not induce the nucleoid condensation in *E. coli*. This implies, in turn, the existence of a log phase specific factor(s) that inhibits the nulceoid condensation under oxidative stress.

Role of Fis on the Dps-induced nucleoid condensation

In *E. coli*, Fis is the most abundant nucleoid component in the log phase ($\sim 60\,000$ molecules/cell), whereas its expression becomes undetectable at the stationary phase (Azam and Ishihama, 1999). When Dps is overexpressed in the wt (fis^+) strain in the log phase, the nucleoid was not condensed (Kim *et al*, 2004). *S. aureus*, in which the expression of MrgA (Dps ortholog) is directly coupled with the nucleoid condensation (Morikawa *et al*, 2006), does not possess *fis* nor its homologous genes (Takeyasu *et al*, 2004). Therefore, we suspect Fis to be an inhibitory factor against the nucleoid condensation. To test this hypothesis, Dps was transiently overexpressed in the log phase of a Δfis strain of *E. coli* using a Dps-expression plasmid, and possible changes of the nucleoid structure were examined by DAPI staining and AFM observation. As expected, the induction of Dps by isopropyl-β-D-thiogalactopyranoside (IPTG) condensed the nucleoid even in the log phase, and the efficiency of cell lysis was decreased to 16% (Figure 3A, B and F) from the original value of 80% (Figure 3A and D). Close observations by AFM revealed that the Δfis strain exhibited the fibrous and condensed nucleoid in the absence and presence of Dps overexpression, respectively (Figure 3E and G).

We further investigated whether or not the nucleoid condensation could be induced in the Δfis strain by oxidative stress. Western blot analyses against Dps showed that a treatment of the Δfis strain with $2\,mM$ H_2O_2 induced as much amount of Dps as in the wt treated with $2\,mM$ H_2O_2 (Figure 3C). On-substrate-lysis treatment of the cells and the subsequent DAPI staining demonstrated that only 18% cells were lysed (Figure 3A and H). A close observation by AFM found that the nucleoid in the Δfis cells was condensed under H_2O_2 treatment (Figure 3I). In the stationary phase of the Δfis cells, Dps was normally expressed (Figure 3C), and the nucleoid was condensed (Figure 3A, J and K). Thus, we concluded that Fis is the inhibitory factor for the Dps-dependent nucleoid condensation in the log phase, but it does not participate in the regulation of the *dps*-gene expression.

Figure 3 The lysis efficiency and the nucleoid architecture of the Δfis strain. (**A**) The efficiency of lysis. The number of lysed cells that dispersed fibers was divided by the total cell number and indicated as percent. The numbers of the cells examined are following (each value separated by slash in parentheses represents the number of cells counted at each independent experiment); the log phase (58/39/45/43), under $2\,mM$ H_2O_2 (56/21/45/35), the stationary phase (125/59/77), the overexpression (76/50/74/40/29). (**B**) Overexpression of Dps by IPTG in the Δfis strain. The expression was detected by antibody against Dps. (**C**) Western blot against Dps in the Δfis strain under three different conditions. (**D**) DAPI image of the Δfis strain in the log phase. (**E**) AFM image of the Δdps strain in the log phase. (**F**) DAPI image of the Δfis strain under overexpression of Dps in the log phase. (**G**) AFM image of the Δfis strain under overexpression of DPS in the log phase. (**H**) DAPI image of the Δfis strain in the log phase treated with $2\,mM$ H_2O_2, (**I**) AFM image of the Δfis strain in the log phase treated with $2\,mM$ H_2O_2, (**J**) DAPI image of the Δfis strain in the stationary phase, (**K**) AFM image of the Δfis strain in the stationary phase. Scale bars: $10\,\mu m$ (D, F, H, J) and $500\,nm$ (E, G, I, K).

Effects of Topo I and DNA gyrase on the Dps-induced nucleoid condensation

Fis is known to work as a transcription regulator for the *topA*, *gyrA* and *gyrB* genes, each coding for Topoisomerase I (Topo I), DNA gyrase subunit A (GyrA) and subunit B (GyrB), respectively (Schneider *et al*, 1999; Weinstein-Fischer *et al*,
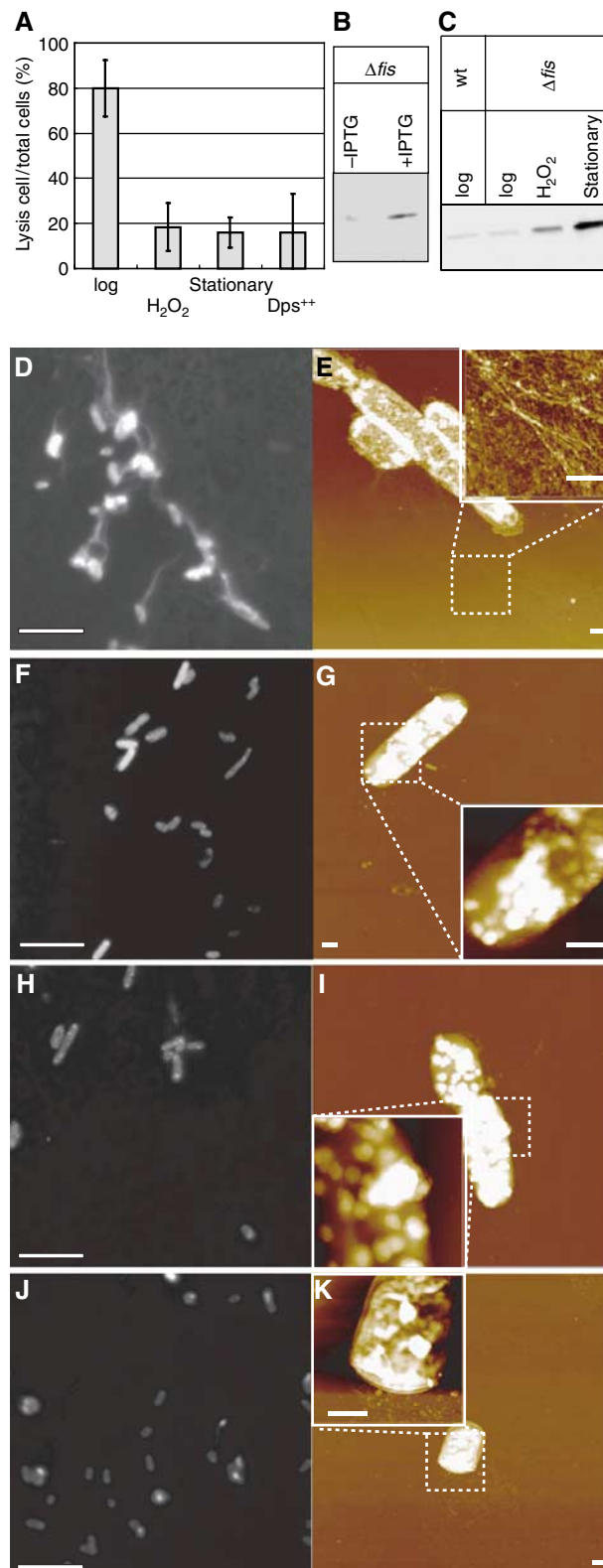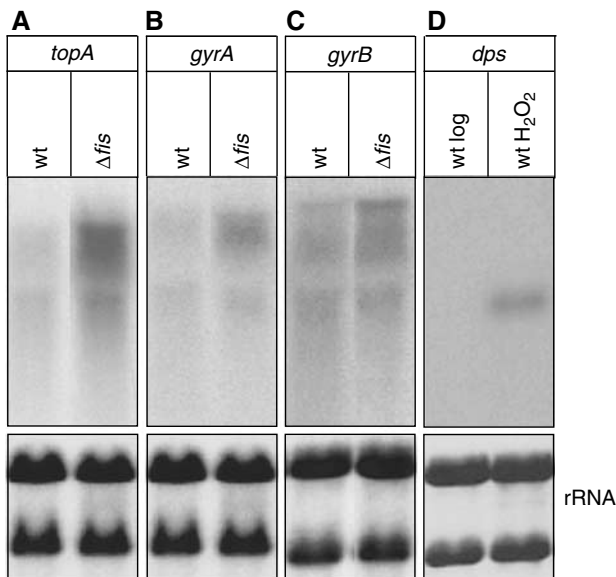
Figure 4 Northern blot analyses of *top A*-, *gyrA*-, *gyrB*- and *dps*-mRNAs. The levels of (**A**) *topA*-, (**B**) *gyrA*- and (**C**) *gyrB*-mRNAs in the wt and Δ*fis* strains. (**D**) The levels of *dps*-mRNAs in the wt cells in the log phase and in the log phase treated with 2 mM H_2O_2. (**A–C**) do not show tight bands, whereas (**D**) shows a single tight band. In bacteria, many mRNAs have been detected as broad smears by Northern blot analyses (Maruyama *et al*, 2003).

2000). Indeed, our Northern blot analysis indicated that the expression of these genes were upregulated in the Δ*fis* strain (Figure 4). Topo I is known to relax supercoiled DNA, whereas DNA gyrase causes negative supercoiling of DNA. Therefore, the repression of nucleoid condensation by Fis might be due to the changes in intracellular levels of Topo I, GyrA and GyrB, ultimately leading to the changes in DNA topology. This interpretation is in good agreement with the fact that the topology control of DNA is critical for achieving the higher-order structures of DNA (Yoshimura *et al*, 2000; Hizume *et al*, 2004; Hizume *et al*, 2005). We examined this possibility by monitoring the *in vivo* status of DNA topology in the wt and Δ*fis* strain. Agarose gel electrophoresis containing chloroquine showed that, in the log phase, the population distribution of supercoiled plasmids was larger in the wt than in Δ*fis* strain, being consistent with our interpretation (Supplementary Figure 1).

We constructed a wt (fis^+) strain that can transiently express His-tagged Topo I, as described in Materials and methods. The induction of His-Topo I expression by IPTG was evidenced by Western blot analysis (Figure 5A). In these His-Topo I expressing cells, the nucleoid was easily dispersed as in the wt cells (Figure 5C). In contrast, when Dps was induced by the treatment with 2 mM H_2O_2 after Topo I induction, the nucleoid became highly condensed (Figure 5D–F). In the cells expressing His-tagged DNA gyrase (GyrA and GyrB) (Figure 5B), the nucleoid without H_2O_2 was easily dispersed (Figure 5G), whereas the nucleoids were also condensed when treated with 2 mM H_2O_2 (Figure 5H–J).

Cell extracts from Δ*fis*, Topo I^{++} and DNA Gyrase^{++} cells control DNA topology

The expression of *gyrA* and *gyrB* is induced by the decrease in negative supercoil in cells (Menzel and Gellert, 1987; Peter
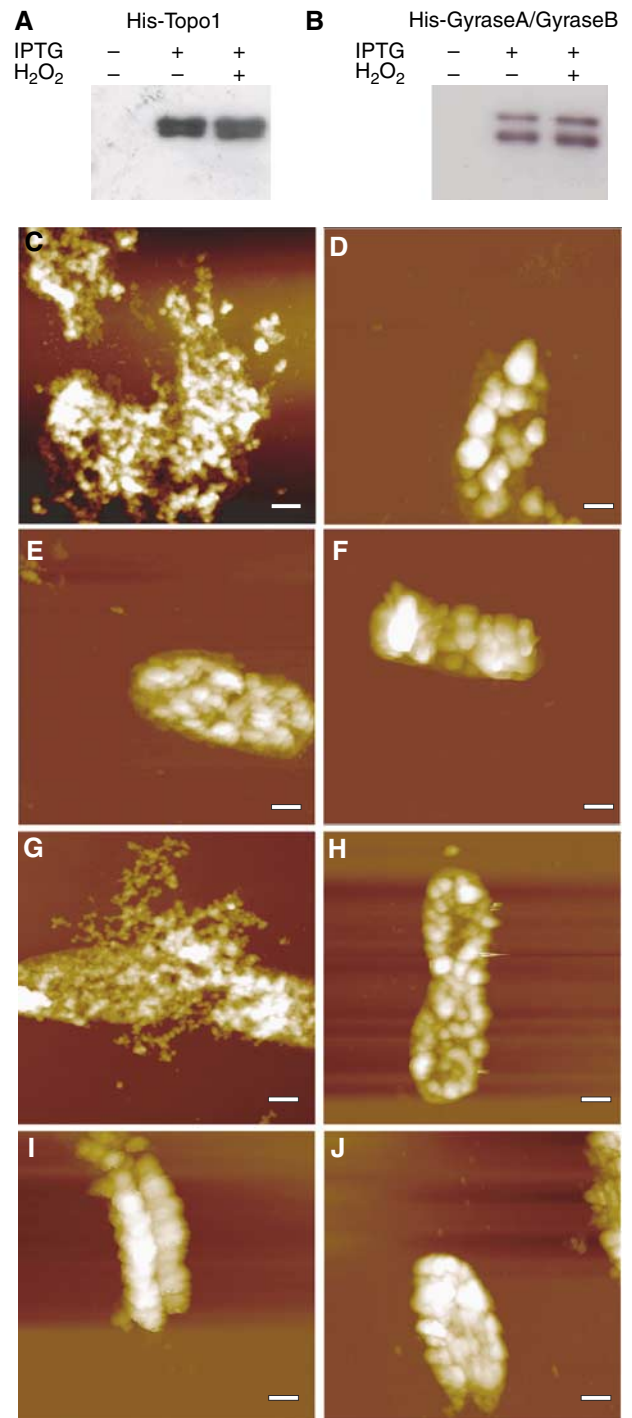

Figure 5 Nucleoid dynamics in Topo I- or DNA gyrase-overexpressing cells. The expression of His-tagged Topo I (**A**) or His-tagged DNA gyrase (**B**) was detected by an antibody against His-tag. (**C**) AFM image of Topo I-overexpressing cell in the log phase, (**D–F**) AFM images of Topo I-overexpressing cells treated with 2 mM H_2O_2, (**G**) AFM image of DNA gyrase-overexpressing cell in the log phase, (**H–J**) AFM image of DNA gyrase-overexpressing cells treated with 2 mM H_2O_2. Scale bars: 500 nm.

et al, 2004), and the increase in negative supercoil facilitates *topA* expression (Menzel and Gellert, 1983; Mizushima *et al*, 1993; Ogata *et al*, 1994). Thus, DNA topology can be controlled by Topo I and GyrA/GyrB in cells. Northern blot analyses indicated that the overexpression of GyrA and

GyrB upregulated the expression level of Topo I, but that the overexpression of Topo I did not change the amount of *gyrA/gyrB* mRNA in our experimental system (Figure 6A–C). In any case, Topo I and DNA gyrase coexist in these overexpressing cells.
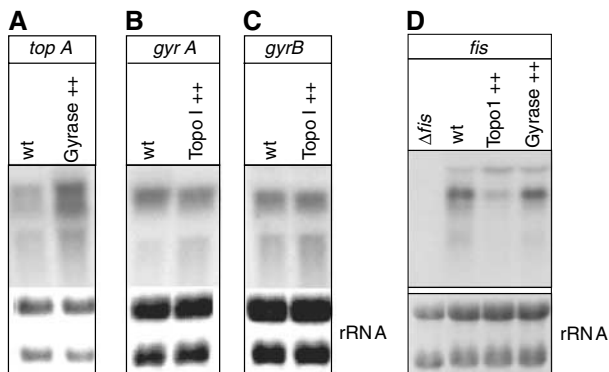

Figure 6 Northern blot analyses of *topA*-, *gyrA*-, *gyrB*- and *fis*-mRNAs under the overexpression of Topo I and DNA gyrase. The levels of (**A**) *topA*-mRNA in DNA gyrase^{++}, (**B, C**) *gyrA*- and *gyrB*-mRNAs in Topo I^{++}, and (**D**) *fis*-mRNA in Topo I^{++} or DNA gyrase^{++}.

To clarify the biological significance, we further examined how efficiently different cell extracts derived from the wt, Δfis and Topo I-/DNA gyrase-overexpressing strains (Topo I^{++} and Gyrase^{++}) could change the topology of DNA *in vitro*. The agarose gel electrophoresis containing chloroquine showed that, whereas wt extract never changed the population of topoisomers of DNA, the extract from Δfis, Topo I^{++} and Gyrase^{++} changed the population toward relaxed form (Figure 7A). These results indicate that the topology of DNA is dynamically transmutable in the Δfis, Topo I^{++} and Gyrase^{++} strains, but not in the wt strain. Also, it is interesting to note that the cell extract from Gyrase^{++} had a very similar effect to that from Topo I^{++}. It seems that the effect of Topo I in the extract predominate over the effect of DNA gyrase, and the effects of DNA gyrases in the extract may be very subtle and involved a local topology control. Indeed, when the extract from Gyrase^{++} was added to the extract from Topo I^{++}, the topoisomers were not shifted toward supercoiling but toward relaxed form (Figure 7B, also see Supplementary Figure 2).

It is well known that DNA gyrase requires ATP and Mg^{2+} for its action. Consequently, we examined the effect of ATP (1~10 mM) and Mg^{2+} (1~100 mM) in the DNA gyrase^{++} cell extracts on the DNA topology. Unexpectedly, the popula-
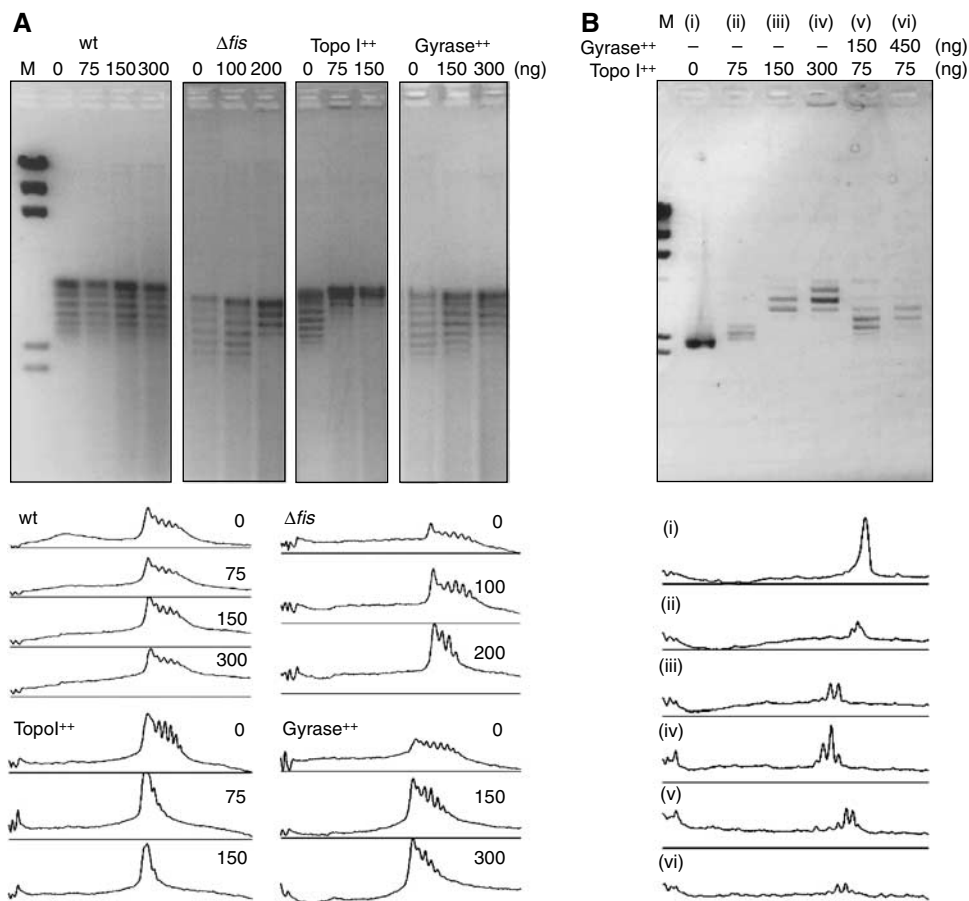

Figure 7 DNA topology assay using Δfis, Topo I^{++} and Gyrase^{++} cell extracts. (**A**) The plasmid DNA (pBSII SK$^-$) was incubated with cell extracts prepared from wt, *fis*-deletion cells (Δfis), Topo I-overexpressed cells (Topo I^{++}) and DNA gyrase-overexpressed cells (Gyrase^{++}) for 15 min at 37°C, and then loaded onto agarose gels containing 2.5 mg/ml chloroquine. (**B**) The extract from Gyrase^{++} was added to the extract from Topo I^{++}, and was incubated with pBSII for 15 min at 37°C. The electrophoresis was performed without chloroquine. M represents the marker DNA (λ DNA digested by *Hin*dIII (BioLabs)), and the numbers above the gels indicate the amounts of proteins in each cell extract (ng). The graphs represent microdensitometric tracings corresponding to the lanes.

tions of topoisomers were shifted toward the relaxed forms in a similar extent to the effect in the absence of ATP and Mg^{2+} (data not shown). It seems that the effect of Topo I predominates over the effect of DNA gyrase.

Discussion

We have previously reported that, in *S. aureus,* the induction of Dps ortholog, MrgA, by oxidative stress induced a nucleoid condensation. The Dps-dependent nucleoid condensation was postulated as the genome protection system against oxidative stress. However, in this study, we demonstrated that the oxidative stress did not simply lead to the nucleoid condensation in *E. coli* due to the effects of Fis as the regulator of the *topA* and *gyrA/B* gene expression that is required for the control of DNA topology.

DNA topology maintenance by Fis, Topo I and DNA gyrase

Fis preferably binds to the 15 bp consensus sequence, but when it exists in excess amount, its DNA-binding becomes sequence nonspecific. *In vitro*, Fis changes the overall shape of supercoiled DNA in a sequence-independent manner (Schneider *et al*, 2001; Hardy and Cozzarelli, 2005), and prevents the topological changes caused by DNA gyrase and Topo I (Schneider *et al*, 1997). In addition, our results showed that Fis repressed the expressions of *gyrA*, *gyrB* and

topA (Figure 4). These facts suggest that Fis plays a role to sustain the DNA superhelicity at the steady-state level using two different pathways: one is acting as a physical barrier and buffering the change in the DNA superhelicity, and the other is repressing the expression of the factors that change the DNA superhelicity (Figure 8A). In fact, the cell extract from the wt (*fis*[+]) strain could not affect the population distribution of topoisomers, whereas the cell extract from the Δ*fis* strain changed the population distribution of the topoisomers (Figure 7).

The DNA topology should be always balanced in a cell. In this sense, all of the following may be critical: (i) direct binding of Fis to DNA and forming a physical barrier (Schneider *et al*, 1997, 2001; Hardy and Cozzarelli, 2005); (ii) controlling gene expression including *topA* and others (Schneider *et al*, 1999; Weinstein-Fischer *et al*, 2000); (iii) ionic environment that directly affect DNA compaction (Iwataki *et al*, 2004). In the Δ*fis* strain, DNA gyrases and Topo I actively change the DNA superhelicity without the barrier of Fis, and the topology of DNA turns into the dynamic state, in which the expression of Dps would easily results in the nucleoid condensation (Figure 8B). This is the case for *S. aureus,* whose MrgA expression and the nucleoid condensation are completely correlated (Morikawa *et al*, 2006). Database search showed that *S. aureus* lacks *fis* gene (Table I), but possess the orthologs of *topA*, *gyrA* and *gyrB*. Namely, the nucleoid dynamics in the wt strain of *S. aureus*
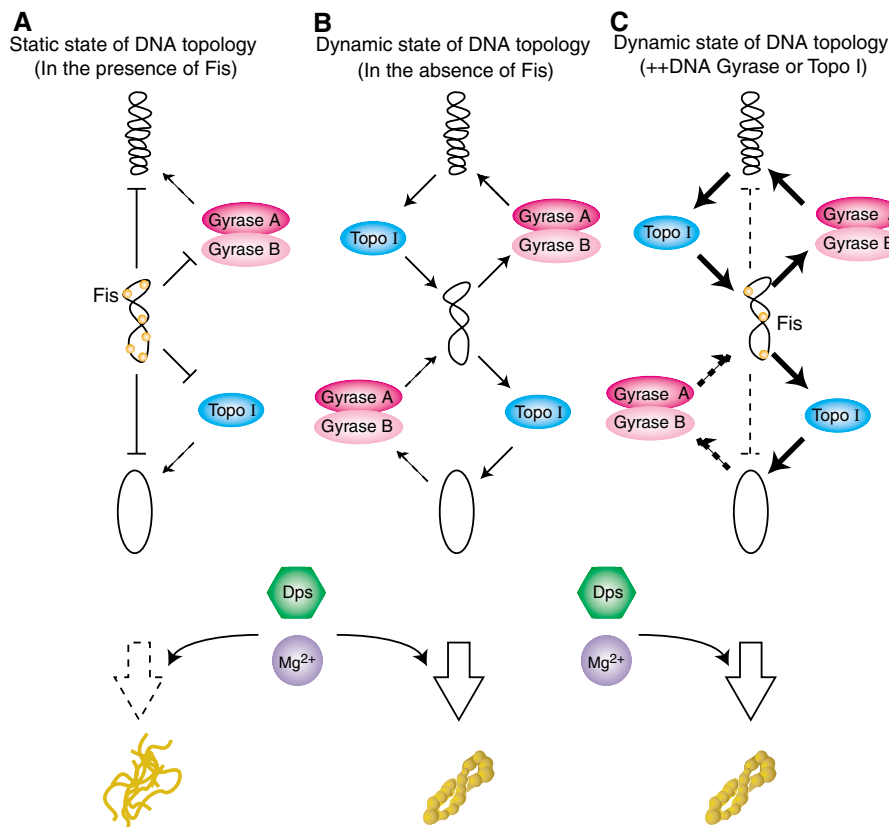

Figure 8 A model of the topology control of genome DNA required for the Dps-dependent nucleoid condensation. (**A**) In the presence of Fis, DNA topology is maintained statically by the repression of Topo I and DNA gyrase expressions, and also by the physical blocking against the topological changes of DNA topoisomers. Therefore, the expression of Dps does not lead to a nucleoid condensation. (**B**) In the absence of Fis, Topo I and DNA gyrase are induced and may easily change the DNA topology. Thus DNA topology is dynamic. This status allows the nucleoid to be condensed under the expression of Dps (Topo I and DNA gyrase coexist). (**C**) Overexpression of Topo I or DNA gyrase may overcome the barrier of Fis, cause the DNA topology dynamic, and facilitate the nucleoid condensation as in (B).

Table I The distribution of Fis, OxyR and PerR, and the potential binding sites of OxyR and PerR on the dps gene in bacterial species possessing Dps

	Gene distribution				Binding sites prediction (bit)	
	DPS	Fis	OxyR	PerR	OxyR	PerR
Proteobacteria						
Gamma						
Escherichia coli K-12 MG1655	+	+	+	−	10.4	10.7
Escherichia coli K-12 W3110	+	+	+	−	10.4	10.7
Escherichia coli O157 EDL933	+	+	+	−	10.4	10.7
Escherichia coli O157 Sakai	+	+	+	−	10.4	10.7
Escherichia coli CFT073	+	+	+	−	10.4	10.7
Salmonella typhi CT18	+	+	+	−	20.1	11
Salmonella typhimurium	+	+	+	−	20.1	11
Yersinia pestis CO92	+	+	+	−	−	9.9
Yersinia pestis KIM	+	+	+	−	−	9.9
Shigella flexneri 301 (serotype 2a)	+	+	+	−	9.5	10.7
Haemophilus influenzae	+	+	+	−	18.2	8.6
Pasteurella multocida	+	+	+	−	21.3	7.7
Xylella fastidiosa 9a5c	+	+	+	−	−	−
Xylella fastidiosa Temecula1	+	+	+	−	−	−
Xanthomonas campestris	+	+	+	−	−	−
Xanthomonas axonopodis	+	+	+	−	−	−
Vibrio cholerae	+	+	+	−	16.7	6.8
Vibrio vulnificus	+	+	+	−	28.5	−
Vibrio parahaemolyticus	+ +	+	+	−	24.4/7.4	13.8/−
Pseudomonas aeruginosa	+	+	+	−	−	−
Shewanella oneidensis	+	+	+	−	12.9	−
Ralstonia solanacearum	+	+	+	−	−	−
Delta/epsilon						
Helicobacter pylori 26695	+	−	−	+	12	9.2
Helicobacter pylori J99	+	−	−	+	12	9.2
Campylobacter jejuni	+	−	−	+	11.2	21.3
Alpha						
Rickettsia prowazekii	+	−	−	−	11.1	9.8
Agrobacterium tumefaciens C58 (UWash/Dupont)	+	−	+	+	−	−
Agrobacterium tumefaciens C58 (Cereon)	+	−	+	+	−	−
Brucella melitensis	+	−	+	+	−	−
Brucella suis	+	−	+	+	−	−
Bradyrhizobium japonicum	+	−	+	+	−	−
Caulobacter crescentus	+	−	+	-	−	−
Firmicutes						
Bacillales						
Bacillus subtilis	+ +	−	−	+	9.8/−	28.1/−
Bacillus halodurans	+	−	−	+	−	−
Bacillus anthracis	+ +	−	−	+	10.9/−	23.1/11.9
Bacillus cereus	+ +	−	−	+	11.5/−	21.6/7.9
Oceanobacillus iheyensis	+	−	−	+	−	−
Staphylococcus aureus N315 (MRSA)	+	−	−	+	8.8	19.3
Staphylococcus aureus Mu50 (VRSA)	+	−	−	+	8.8	19.3
Staphylococcus aureus MW2	+	−	−	+	8.8	19.3
Staphylococcus epidermidis	+	−	−	+	5.1	25.3
Listeria monocytogenes	+	−	−	+	−	17.4
Listeria innocua	+	−	−	+	−	17.4
Lactobacillales						
Lactococcus lactis	+	−	−	+	−	7.5
Streptococcus pyogenes SF370 (serotype M1)	+	−	−	+	−	6.6
Streptococcus pyogenes MGAS8232 (serotype M18)	+	−	−	+	−	6.6
Streptococcus pyogenes MGAS315 (serotype M3)	+	−	−	+	−	6.6
Streptococcus pneumoniae TIGR4	+	−	−	−	−	−
Streptococcus pneumoniae R6	+	−	−	−	−	−
Streptococcus mutans	+	−	−	+	15.2	12.1
Lactobacillus plantarum	+	−	−	+	−	7.7
Enterococcus faecalis	+ +	−	−	+	6.1/−	14.4/7.5
Clostridium tetani	+	−	−	+	12	12.7
Actinobacteria						
Mycoplasma pulmonis	+	−	−	−	10	15
Corynebacterium glutamicum	+	−	+	−	−	−
Corynebacterium efficiens	+	−	+	−	−	5.2
Streptomyces coelicolor	+	−	+	+	−	−
Bifidobacterium longum	+	−	−	−	−	−
Tropheryma whipplei Twist	+	−	−	−	−	−
Tropheryma whipplei TW08/27	+	−	−	−	−	−

Table I Continued

	Gene distribution				Binding sites prediction (bit)	
	DPS	Fis	OxyR	PerR	OxyR	PerR
Fusobacteria						
Fusobacterium nucleatum	+	−	−	+	9.2	20.0
Spirochete						
Borrelia burgdorferi	+	−	−	+	8.0	10.8
Treponema pallidum	+	−	−	−	−	−
Leptospira interrogans	+	−	−	+	7.5	5.1
Cyanobacteria						
Synechocystis sp. PCC6803	+	−	−	+	−	−
Thermosynechococcus elongatus	+	−	−	−	−	8.0
Anabaena sp. PCC7120 (Nostoc sp. PCC7120)	+ + +	−	−	−	6.4/5.6/−/−	11.9/−/−/−
Radioresistant bacteria						
Deinococcus radiodurans	+	−	−	−	−	−

The presence and absence of the proteins is shown by + and − respectively.
The number of + represents the number of closely related homologs in a certain species.
The value in the column of the potential binding sites of OxyR and PerR indicates the information amount of the respective binding sites (bit).

correspond to those in the *E. coli* Δ*fis* strain (Figure 8B). Taken together, the topology control of DNA seems to be critical for the Dps-dependent nucleoid condensation.

A binding of Fis to DNA may physically block the interaction between DNA and Dps, because Fis binds to DNA in a sequence nonspecific manner (Schneider *et al*, 2001). However, since the amount of Fis in a cell in the log phase is ∼60 000 (Azam and Ishihama, 1999) and Fis functions as a homo-dimer (Kostrewa *et al*, 1992), the amount of Fis may not be sufficient to physically block the entire genomic DNA from Dps (∼1 Fis dimer per 150 bp genome DNA, genome size = 4.6 Mbp). In the Topo I^{++} and Gyrase^{++} cells with an ability of immediate nucleoid compaction upon H_2O_2 stimulation, the mRNA of *fis* was still present (Figure 6D). Therefore, the dynamics of nucleoid structure is likely controlled on the balance of the effects of Fis, Topo I, DNA gyrase and Dps, but not simply by a physical blocking (Figure 8C). The fact that the extracts from Topo I^{++} and Gyrase^{++} cell changed the topology of DNA supports this idea (Figure 7).

The relationship between DNA–Dps crystallization and nucleoid condensation

It has been reported that DNA–Dps interaction and the following DNA–Dps crystallization are independent of DNA superhelicity *in vitro* (Almiron *et al*, 1992; Wolf *et al*, 1999; Frenkiel-Krispin *et al*, 2004). *In vitro* reconstitution of nucleosomes can also be done on a linear and relatively short DNA. However, although a nucleosome on a short linear DNA winds ∼146 bp of DNA, the efficiency on a long (∼100 kb) DNA is strongly depending on the superhelicity of the DNA (Hizume *et al*, 2004, 2005). In this study, we are dealing with the entire genome (∼4 Mbp). Therefore, the implication obtained from *in vitro* experiments may not be simply applicable to a much larger *in vivo* system, and thus, it is speculated that the topology control may be critical for the DNA–Dps crystallization when it comes to the entire genome.

The concentration of doubly charged cations has been known to contribute to the DNA–Dps interaction and crystallization (Grant *et al*, 1998; Frenkiel-Krispin *et al*, 2001), being particularly important as a regulating signal for DNA–Dps

interaction upon entry to the stationary phase (Hurwitz and Rosano, 1967). Therefore, such divalent cations are also expected to be critical for Dps-dependent nucleoid condensation on the balance of the topological state of genome DNA. Since the overexpression of Dps in the log phase of wt never exposes the DNA–Dps crystalline state, the cation-facilitated conformational change of the genome DNA might be required for bridging the DNA–Dps crystalline to the genome condensation towards stationary phase. Although at present, unfortunately, little information about the concentration of divalent cations is available for the log phase, toward the stationary phase, the genome DNA in *E. coli* is restructured and formed toroidal morphology inside the Dps crystal in a cell (Frenkiel-Krispin *et al*, 2004).

Different response to oxidative stress via Dps induction in bacteria

We have previously reported that the *dps* gene is present widely in the bacterial kingdom (Kim *et al*, 2004; Takeyasu *et al*, 2004), and that it is generally induced in response to oxidative stresses through different transcription factors (Morikawa *et al*, 2006). One of them is OxyR, which is present in gamma-Proteobacteria including *E. coli*, beta-Proteobacteria, alpha-Proteobacteria and Actinobacteria (Table I). Another is PerR, which is functional counterpart of OxyR and works as a repressor for the *mrgA* gene (Horsburgh *et al*, 2001, 2002; Morikawa *et al*, 2006). PerR is distributed in Firmicutes including *S. aureus*, Spirochete, Cyanobacteria, Hyperthermophilic bacteria, alpha-Proteobacteria and Chlamidia (Table I). Since there is no primary-sequence homology between PerR and OxyR, these two regulatory systems seem to have evolved independently. We have previously speculated that bacterial species that possess the *dps* gene have an ability to compact their nucleoid under oxidative stress, since *S. aureus* expresses MrgA under oxidative stress and condenses its nucleoid (Morikawa *et al*, 2006). However, in this study, we found that, due to the presence of Fis, the nucleoid in *E. coli* could not be condensed under oxidative stress that induced the Dps expression. In this case, timely expression of Dps as the Fe-chelater (or

ferroxidase) may have a role in inhibiting the production of hydroxyl radicals under oxidative stress.

We re-compared the distributions between Fis and the transcription regulators of the *dps* gene in bacterial kingdom in terms of the nucleoid condensation sensitive to the oxidative stress. In order to precisely predict the actual involvement of OxyR and PerR, we applied the Schneider's information theory (Hengen *et al*, 1997; Schneider, 1997; Zheng *et al*, 2001). We explored the binding sites of OxyR and PerR on the promoter regions of *dps* and *dps* homologs throughout the bacterial kingdom (Table I). A comparison of the binding sites with their corresponding regulators revealed that the regulation system of *dps* by OxyR exists only in gamma-Proteobacteria including *E. coli*, although OxyR itself is distributed in gamma-Proteobacteria, alpha-Proteobacteria and Actinobacteria. The distribution of Fis is also restricted in gamma-Proteobacteria, suggesting that the Dps induction by oxidative stress in gamma-Proteobacteria, in general, does not lead to a nucleoid condensation. In contrast, the PerR system is distributed not only in *Bacillales* including *S. aureus* but also in *Lactobacillales*, delta/epsilon-Protebacteria, Fusobacteria, Spirochete and Cyanobacteria, indicating that the regulation of *dps* expression by PerR is more universal in bacteria and, therefore, seems to be the older system than by OxyR. Since the distribution of PerR system never overlaps with the presence of Fis, the species possessing the PerR system will induce an immediate nucleoid condensation under oxidative stress. From this sense, it is likely that the protection system of genome DNA against oxidative stress without nucleoid condensation have been developed specifically in gamma-Proteobacteria, coupled with the later acquisitions of Fis and the OxyR dependent regulation of the *dps* gene.

Materials and methods

Bacterial strain and growth condition

wt (W3110) and the *dps* deletion mutant (W3110 (Δ*dps::Km*)) are *E. coli* K-12 derived strain (Kim *et al*, 2004). The *oxyR*, *himD* (*ihf-B*) and *fis* deletion mutants (K-12 BW25113 derived strains) were obtained from the KO collection (systematic knock out strain of *E. coli* K-12; GenoBase: http://ecoli.aist-nara.ac.jp/) by Baba *et al* (2006). P1 vir phages were prepared from these deletion mutants as donors. Thereafter deletion mutants of W3110 (Δ*oxyR::Km*, Δ*himD::Km* and Δ*fis::Km*) were constructed by P1 general transduction using the recipient strain W3110 (wt). Glycerol stocks of W3110 strains (wt, Δ*dps*, Δ*oxyR*, Δ*himD* (*ihf-B*) and Δ*fis*) were inoculated into LB medium and cultured at 37°C with constant shaking (180 r.p.m., Bioshaker BR-15 (TAITEC)) for 24 h. Ten microliters of the saturated culture were inoculated into 5 ml of fresh LB medium and cultured at 37°C with constant shaking (180 r.p.m., Bioshaker BR-15) to an appropriate cell density. The cell density was determined by measuring the absorbance at 600 nm by UV-160A (Simadzu).

Western blot analysis

Each strain was grown in LB medium until the optical density (OD$_{600}$) reached at 0.5 (log phase) and 2.0 (stationary phase) and was exposed to 2 mM H$_2$O$_2$ for 15 min. After 15-min incubation at 37°C, the cells were harvested by a centrifugation at 13 000 g for 30 s at 4°C, suspended in an SDS sample buffer (50 mM Tris–HCl pH 6.8, 2% SDS, 1% 2-mercaptoethanol, 10% glycerol, 0.025% bromophenol blue). An equal amount of the cell lysate measured by OD$_{600}$ was subjected to SDS–PAGE and analyzed by immunoblotting with a polyclonal antibody against Dps. Specific binding was detected with ECL-labeled secondary antibody.

Northern blot analysis

Every strain was grown in LB medium until the OD$_{600}$ reached at 0.5 (log phase), and was exposed to the 2 mM H$_2$O$_2$. After 15 min incubation, the cells were harvested by a centrifugation at 13 000 g for 30 s at 4°C, suspended in a lysis buffer containing 10 mM Tris–Cl (pH 8.0), 10 mM EDTA and 400 μg/ml of lysozyme, and, then, incubated at 37°C for 2 min. The total RNA was extracted from the lysate by the SV total RNA isolation system (Promega). Four micrograms of the total RNAs was separated on a 1% agarose-formamide denaturing gel and transferred onto the Hybond N$^+$ membrane (Amersham Biosciences). The DNA fragments prepared by PCR from the W3110 genomic DNA were labeled by a random priming method using the Ready-to-Go DNA labeling Beads (Amersham Biosciences), and used as the probes. The hybridization was conducted at 60°C in the hybridization solution containing 5 × SSPE, 5 × Denhardt's solution, 0.5% SDS and 20 μg/ml of salmon sperm DNA for 16 h, and the final washing was carried out at 60°C in 0.1 × SSC and 0.1% SDS for 30 min.

'On-substrate lyses' procedure

Bacterial cells were harvested from 100 μl culture by centrifugation (13 000 g, 1 min at 4°C) and washed once with 1 ml phosphate-buffered saline (PBS) (pH 7.2). The cells were resuspended in 250 μl of PBS and a 50 μl aliquot was placed onto a round-shape cover glass of 15 mm in diameter. The extra liquid was removed by nitrogen gas blow. Each strain was immersed in 2 ml of a buffer containing 10 mM Tris–HCl (pH 8.2), 1 mM NaN$_3$ and 0.1 M NaCl for 5 min, followed by an addition of 25 μg/ml lysozyme. After 2 min incubation at 25°C, Brij 58 (polyoxyethylene hexadecyl ether) and sodiumdeoxycholate were added to the final concentrations of 0.25 and 0.1 mg/ml, respectively. After 10 min, the cover glass was dried under nitrogen gas. The surface of the cover glass was gently washed with distilled water and dried again for AFM analyses. For the observation by fluorescent microscopy (Axiobert 200, Olympus), the sample was stained by DAPI.

AFM analyses

The atomic force microscope (SPI3800N-SPA400) from Digital Instrument was used for the imaging of *E. coli* nucleoid structures in air at room temperature under a tapping mode with a 100 μm scanner. Probes made of a single silicon crystal with the cantilever length of 129 μm and the spring constant of 33–62 N/m (OMCL-AC160TS-W2, Olympus) were used for imaging. Data were collected in the height mode with a scanning rate of 0.5–1.0 Hz and the driving amplitude of 40–80 mV. The images were captured in a 512 × 512 pixels format and the captured images were flattened and plane-fitted before analysis. The image analyses were performed with the software accompanying with the imaging module.

All of the AFM images contain 'tip effect'. The sizes of the objects in the images were estimated at the half-maximum height (FWHM, full-width at half-maximum) for correction of the tip effect (Schneider *et al*, 1998). In the present study, we have found that the AFM cantilevers purchased from Olympus had a constant tip angle of ∼35°, and a tip radius of 5±2 nm by measuring the apparent width of double-stranded DNA in the AFM images.

Overexpression of Dps, Topo I and DNA gyrase in the wt and the Δfis strain

The coding sequences for the Dps, Topo I, DNA gyrase subunit A and subunit B was amplified by PCR and subcloned into the pCA24N vector (28), which contained the sequences for the green fluorescent protein (GFP) and 5xHis. The GFP sequence in the pCA24N vector was deleted by *Sal*I restriction enzyme. The *dps*, *topA*, *gyrA* and *gyrB* genes are now under the control of the pT5/lac promoter. For the co-expression of *gyrA* and *gyrB* in W3110, *gyrB* gene was subcloned into RSFDuet-1 (Novagen). The gene expressions of *topA* and *gyrA/B* can be induced by IPTG. The plasmid DNA was then transformed into a *fis*-deletion strain and the wt of W3110. The cells at different growth phases were exposed to IPTG (0.5 mM) for varying periods of time and subjected to Western blot and AFM analyses.

Topology assay of plasmid DNA

Cytosol extracts were prepared as following. Twenty-five milliliters of bacterial cultures in the log phase (OD$_{600}$, 0.5) were harvested by

centrifugation at 5000 *g* for 10 min, and the bacterial pellets were resuspended in 1 ml buffer P (PBS + 1 mM PMSF and protein inhibitor cocktail (Nakarai)). Lysozyme was added to the final concentration of 25 μg/ml, and incubated on ice for 30 min. After centrifugation at 5000 *g* for 10 min, glycerol (final concentration is 5%) was added to the supernatants (cell extracts), and the extracts were stored at −20°C. The amount of proteins in the cell extracts was determined by DC protein assay kit (Lowly method, BIO-RAD).

pBluescript SKII-(pBSII) was purified from the stationary phase culture (overnight culture) by midi-prep kit (Qiagen). The cell extracts were added to 500 ng pBSII and incubated at 37°C for 15 min. The reaction was stopped by the addition of 1% SDS. Following phenol/chloroform extraction, the plasmid sample was collected by ethanol precipitation, resuspended in TE with 1 μg/ml RNase, and loaded into a 1.2% agarose gel containing 0.25 μg/ml chloroquine (Shure *et al*, 1977). Electrophoresis was performed in TAE buffer containing 0.25 μg/ml chloroquine for 15–17 h at 25 V in a refrigerator. The gels were washed with distilled water for 4 h, stained with EtBr for 2 h, and observed by FAS-II (TOYOBO).

Information analysis of the IHF, OxyR and PerR binding sites on the dps gene promoter

Fifty-one and nineteen known OxyR and PerR binding sites were collected, respectively, and each individual information weight matrix in a set of the binding sites was constructed according to the Schneider's information theory (Schneider, 1997). Then the matrix was applied to the promoter regions (−200 ∼ −1) of 76 *dps* genes in 68 bacterial species, which had been known to posses the *dps* gene (Morikawa *et al*, 2006), and the information contents in each promoter were calculated. The scores in Table I represent the highest scores in a certain *dps* promoter.

Supplementary data

Supplementary data are available at *The EMBO Journal* Online (http://www.embojournal.org).

Acknowledgements

References

Almiron M, Link AJ, Furlong D, Kolter R (1992) A novel DNA-binding protein with regulatory and protective roles in starved *Escherichia coli*. *Genes Dev* **6:** 2646–2654

Altuvia S, Almiron M, Huisman G, Kolter R, Storz G (1994) The dps promoter is activated by OxyR during growth and by IHF and sigma S in stationary phase. *Mol Microbiol* **13:** 265–272

Azam TA, Ishihama A (1999) Twelve species of the nucleoid-associated protein from *Escherichia coli*. Sequence recognition specificity and DNA binding affinity. *J Biol Chem* **274:** 33105–33113

Azam TA, Hiraga S, Ishihama A (2000) Two types of localization of the DNA-binding proteins within the *Escherichia coli* nucleoid. *Genes Cells* **5:** 613–626

Baba T, Ara T, Hasegawa M, Takai Y, Okumura Y, Baba M, Datsenko KA, Tomita M, Wanner BL, Mori H (2006) Construction of *Escherichia coli* K-12 in-frame, single-gene knockout mutants: the Keio collection. *Mol Systems Biol* **2:** 2006.0008

Choi SH, Baumler DJ, Kaspar CW (2000) Contribution of dps to acid stress tolerance and oxidative stress tolerance in *Escherichia coli* O157:H7. *Appl Environ Microbiol* **66:** 3911–3916

Frenkiel-Krispin D, Ben-Avraham I, Englander J, Shimoni E, Wolf SG, Minsky A (2004) Nucleoid restructuring in stationary-state bacteria. *Mol Microbiol* **51:** 395–405

Frenkiel-Krispin D, Levin-Zaidman S, Shimoni E, Wolf SG, Wachtel EJ, Arad T, Finkel SE, Kolter R, Minsky A (2001) Regulated phase transitions of bacterial chromatin: a non-enzymatic pathway for generic DNA protection. *EMBO J* **20:** 1184–1191

Grant RA, Filman DJ, Finkel SE, Kolter R, Hogle JM (1998) The crystal structure of Dps, a ferritin homolog that binds and protects DNA. *Nat Struct Biol* **5:** 294–303

Hardy CD, Cozzarelli NR (2005) A genetic selection for supercoiling mutants of *Escherichia coli* reveals proteins implicated in chromosome structure. *Mol Microbiol* **57:** 1636–1652

Hayat MA, Mancarella DA (1995) Nucleoid proteins. *Micron* **26:** 461–480

Hengen PN, Bartram SL, Stewart LE, Schneider TD (1997) Information analysis of Fis binding sites. *Nucleic Acids Res* **25:** 4994–5002

Hizume K, Yoshimura SH, Takeyasu K (2004) Atomic force microscopy demonstrates a critical role of DNA superhelicity in nucleosome dynamics. *Cell Biochem Biophys* **40:** 249–262

Hizume K, Yoshimura SH, Takeyasu K (2005) Linker histone H1 *per se* can induce three-dimensional folding of chromatin fiber. *Biochemistry* **44:** 12978–12989

Horsburgh MJ, Clements MO, Crossley H, Ingham E, Foster SJ (2001) PerR controls oxidative stress resistance and iron storage proteins and is required for virulence in *Staphylococcus aureus*. *Infect Immun* **69:** 3744–3754

Horsburgh MJ, Wharton SJ, Karavolos M, Foster SJ (2002) Manganese: elemental defence for a life with oxygen. *Trends Microbiol* **10:** 496–501

Hurwitz C, Rosano CL (1967) The intracellular concentration of bound and unbound magnesium ions in *Escherichia coli*. *J Biol Chem* **242:** 3719–3722

Iwataki T, Kidoaki S, Sakaue T, Yoshikawa K, Abramchuk SS (2004) Competition between compaction of single chains and bundling of multiple chains in giant DNA molecules. *J Chem Phys* **120:** 4004–4011

Kim J, Yoshimura SH, Hizume K, Ohniwa RL, Ishihama A, Takeyasu K (2004) Fundamental structural units of the *Escherichia coli* nucleoid revealed by atomic force microscopy. *Nucleic Acids Res* **32:** 1982–1992

Kornberg RD (1974) Chromatin structure: a repeating unit of histones and DNA. *Science* **184:** 868–871

Kostrewa D, Granzin J, Stock D, Choe HW, Labahn J, Saenger W (1992) Crystal structure of the factor for inversion stimulation FIS at 2.0 A resolution. *J Mol Biol* **226:** 209–226

Ljungman M (1991) The influence of chromatin structure on the frequency of radiation-induced DNA strand breaks: a study using nuclear and nucleoid monolayers. *Radiat Res* **126:** 58–64

Ljungman M, Hanawalt PC (1992) Efficient protection against oxidative DNA damage in chromatin. *Mol Carcinogen* **5:** 264–269

Lomovskaya OL, Kidwell JP, Matin A (1994) Characterization of the sigma 38-dependent expression of a core *Escherichia coli* starvation gene, *pexB*. *J Bacteriol* **176:** 3928–3935

Martinez A, Kolter R (1997) Protection of DNA during oxidative stress by the nonspecific DNA-binding protein Dps. *J Bacteriol* **179:** 5188–5194

Maruyama A, Kumagai Y, Morikawa K, Taguchi K, Hayashi H, Ohta T (2003) Oxidative-stress-inducible qorA encodes an NADPH-dependent quinone oxidoreductase catalysing a one-electron reduction in *Staphylococcus aureus*. *Microbiology* **149:** 389–398

Menzel R, Gellert M (1983) Regulation of the genes for E. coli DNA gyrase: homeostatic control of DNA supercoiling. *Cell* **34:** 105–113

Menzel R, Gellert M (1987) Fusions of the *Escherichia coli* gyrA and gyrB control regions to the galactokinase gene are inducible by coumermycin treatment. *J Bacteriol* **169:** 1272–1278

Mizushima T, Natori S, Sekimizu K (1993) Relaxation of supercoiled DNA associated with induction of heat shock proteins in *Escherichia coli*. *Mol Gen Genet* **238:** 1–5

Morikawa K, Ohniwa RL, Kim J, Maruyama A, Ohta T, Takeyasu K (2006) Bacterial nucleoid dynamics: oxidative stress response in *Staphylococcus aureus*. *Genes Cells* **11:** 409–423

Nair S, Finkel SE (2004) Dps protects cells against multiple stresses during stationary phase. *J Bacteriol* **186:** 4192–4198

Nilsson L, Vanet A, Vijgenboom E, Bosch L (1990) The role of FIS in trans activation of stable RNA operons of *E. coli. EMBO J* **9:** 727–734

Nunoshiba T, Obata F, Boss AC, Oikawa S, Mori T, Kawanishi S, Yamamoto K (1999) Role of iron and superoxide for generation of hydroxyl radical, oxidative DNA lesions, and mutagenesis in *Escherichia coli. J Biol Chem* **274:** 34832–34837

Ogata Y, Mizushima T, Kataoka K, Miki T, Sekimizu K (1994) Identification of DNA topoisomerases involved in immediate and transient DNA relaxation induced by heat shock in *Escherichia coli. Mol Gen Genet* **244:** 451–455

Peter BJ, Arsuaga J, Breier AM, Khodursky AB, Brown PO, Cozzarelli NR (2004) Genomic transcriptional response to loss of chromosomal supercoiling in *Escherichia coli. Genome Biol* **5:** R87

Poplawski A, Bernander R (1997) Nucleoid structure and distribution in thermophilic Archaea. *J Bacteriol* **179:** 7625–7630

Robinow C, Kellenberger E (1994) The bacterial nucleoid revisited. *Microbiol Rev* **58:** 211–232

Ross W, Thompson JF, Newlands JT, Gourse RL (1990) *E. coli* Fis protein activates ribosomal RNA transcription *in vitro* and *in vivo. EMBO J* **9:** 3733–3742

Schneider R, Lurz R, Luder G, Tolksdorf C, Travers A, Muskhelishvili G (2001) An architectural role of the *Escherichia coli* chromatin protein FIS in organising DNA. *Nucleic Acids Res* **29:** 5107–5114

Schneider R, Travers A, Kutateladze T, Muskhelishvili G (1999) A DNA architectural protein couples cellular physiology and DNA topology in *Escherichia coli. Mol Microbiol* **34:** 953–964

Schneider R, Travers A, Muskhelishvili G (1997) FIS modulates growth phase-dependent topological transitions of DNA in *Escherichia coli. Mol Microbiol* **26:** 519–530

Schneider SW, Larmer J, Henderson RM, Oberleithner H (1998) Molecular weights of individual proteins correlate with molecular volumes measured by atomic force microscopy. *Pflugers Arch* **435:** 362–367

Schneider TD (1997) Information content of individual genetic sequences. *J Theor Biol* **189:** 427–441

Shure M, Pulleyblank DE, Vinograd J (1977) The problems of eukaryotic and prokaryotic DNA packaging and *in vivo* conformation posed by superhelix density heterogeneity. *Nucleic Acids Res* **4:** 1183–1205

Swedlow JR, Hirano T (2003) The making of the mitotic chromosome: modern insights into classical questions. *Mol Cell* **11:** 557–569

Takeyasu K, Kim J, Ohniwa RL, Kobori T, Inose Y, Morikawa K, Ohta T, Ishihama A, Yoshimura SH (2004) Genome architecture studied by nanoscale imaging: analyses among bacterial phyla and their implication to eukaryotic genome folding. *Cytogenet Genome Res* **107:** 38–48

Thoma F, Koller T, Klug A (1979) Involvement of histone H1 in the organization of the nucleosome and of the salt-dependent superstructures of chromatin. *J Cell Biol* **83:** 403–427

Weinstein-Fischer D, Elgrably-Weiss M, Altuvia S (2000) *Escherichia coli* response to hydrogen peroxide: a role for DNA supercoiling, topoisomerase I and Fis. *Mol Microbiol* **35:** 1413–1420

Widom J, Klug A (1985) Structure of the 300A chromatin filament: X-ray diffraction from oriented samples. *Cell* **43:** 207–213

Wolf SG, Frenkiel D, Arad T, Finkel SE, Kolter R, Minsky A (1999) DNA protection by stress-induced biocrystallization. *Nature* **400:** 83–85

Xu J, Johnson RC (1995) Identification of genes negatively regulated by Fis: Fis and RpoS comodulate growth-phase-dependent gene expression in *Escherichia coli. J Bacteriol* **177:** 938–947

Yoshikawa Y, Hizume K, Oda Y, Takeyasu K, Araki S, Yoshikawa K (2006) Protective effect of vitamin c against double-strand breaks in reconstituted chromatin visualized by single-molecule observation. *Biophys J* **90:** 993–999

Yoshimura SH, Kim J, Takeyasu K (2003) On-substrate lysis treatment combined with scanning probe microscopy revealed chromosome structures in eukaryotes and prokaryotes. *J Electron Microsc (Tokyo)* **52:** 415–423

Yoshimura SH, Ohniwa RL, Sato MH, Matsunaga F, Kobayashi G, Uga H, Wada C, Takeyasu K (2000) DNA phase transition promoted by replication initiator. *Biochemistry* **39:** 9139–9145

Zhao G, Ceci P, Ilari A, Giangiacomo L, Laue TM, Chiancone E, Chasteen ND (2002) Iron and hydrogen peroxide detoxification properties of DNA-binding protein from starved cells. A ferritin-like DNA-binding protein of *Escherichia coli. J Biol Chem* **277:** 27689–27696

Zheng M, Wang X, Doan B, Lewis KA, Schneider TD, Storz G (2001) Computation-directed identification of OxyR DNA binding sites in *Escherichia coli. J Bacteriol* **183:** 4571–4579